



UNIVERSITY
OF WOLLONGONG
AUSTRALIA

University of Wollongong
Research Online

Faculty of Engineering and Information Sciences -
Papers: Part A

Faculty of Engineering and Information Sciences

2013

Organ point dose measurements in clinical multi slice computed tomography (MSCT) examinations with the MOSkin™ radiation dosimeter

C P. L Lian

University of Wollongong, pll098@uowmail.edu.au

A Young

St Vincent's Hospital Sydney

D Cutajar

University of Wollongong, deanc@uow.edu.au

N Freeman

St. Vincent's Hospital, Sydney

Anatoly B. Rosenfeld

University of Wollongong, anatoly@uow.edu.au

Publication Details

Lian, C. P. L., Young, A., Cutajar, D., Freeman, N. & Rozenfeld, A. B. (2013). Organ point dose measurements in clinical multi slice computed tomography (MSCT) examinations with the MOSkin™ radiation dosimeter. *Radiation Measurements*, 55 56-59.

Research Online is the open access institutional repository for the University of Wollongong. For further information contact the UOW Library:
research-pubs@uow.edu.au

Organ point dose measurements in clinical multi slice computed tomography (MSCT) examinations with the MOSkin™ radiation dosimeter

Abstract

This study reports on the application of the MOSkin™ dosimeter in MSCT imaging for the real-time measurement of absorbed organ point doses in a tissue-equivalent female anthropomorphic phantom. MOSkin™ dosimeters were placed within the phantom to measure absorbed point organ doses for 2 commonly applied clinical scan protocols, namely the renal calculus scan and the pulmonary embolus scan. Measured organ doses in the imaged field of view were found to be in the dose range 4.7-9.5 mGy and 16.2-27.4 mGy for the renal calculus scan and pulmonary scan protocols respectively. For the derivation of effective dose, using the more recent ICRP 103 tissue weighting factors (w_T) compared to that of the ICRP 60 w_T resulted in a difference in the derived effective dose by up to 0.8 mSv (-20%) in the renal calculus protocol and up to 1.8 mSv (18%) in the pulmonary embolus protocol. This difference is attributed to the reduced radiosensitivity of the gonads and the increased radiosensitivity of breast tissue in the latest ICRP 103 assigned w_T . The results of this study show that the MOSkin™ dosimeter is a useful real-time tool for the direct assessment of organ doses in clinical MSCT examinations. © 2012 Elsevier Ltd. All rights reserved.

Keywords

dose, point, organ, measurements, clinical, dosimeter, multi, slice, computed, tomography, msct, examinations, moskin, radiation

Disciplines

Engineering | Science and Technology Studies

Publication Details

Lian, C. P. L., Young, A., Cutajar, D., Freeman, N. & Rozenfeld, A. B. (2013). Organ point dose measurements in clinical multi slice computed tomography (MSCT) examinations with the MOSkin™ radiation dosimeter. *Radiation Measurements*, 55 56-59.

Organ Point Dose Measurements in Clinical Multi Slice Computed Tomography (MSCT) examinations with the MOSkinTM Radiation Dosimeter

C.P.L. Lian^{a,*}, A. Young^b, D. Cutajar^a, N. Freeman^c, A.B. Rosenfeld^a

^aCentre for Medical Radiation Physics, Dept of Engineering Physics, Faculty of Engineering, University of Wollongong, Wollongong NSW 2522, Australia

*Corresponding author Tel: + 612 4221 3507; Fax: +612 4221 5474 Email: pll098@uowmail.edu.au

^b St Vincent's Hospital, Department of Nuclear Medicine and PET, Sydney NSW 2010, Australia

^c St Vincent's Hospital, Department of Radiation Oncology, Sydney NSW 2010, Australia

Abstract

This study reports on the application of the MOSkinTM dosimeter in MSCT imaging for the real-time measurement of absorbed organ point doses in a tissue-equivalent female anthropomorphic phantom. MOSkinTM dosimeters were placed within the phantom to measure absorbed point organ doses for 2 commonly applied clinical scan protocols, namely the renal calculus scan and the pulmonary embolus scan. Measured organ doses in the imaged field of view were found to be in the dose range 4.7 to 9.5 mGy and 16.2 to 27.4 mGy for the renal calculus scan and pulmonary scan protocols respectively. For the derivation of effective dose, using the more recent ICRP 103 tissue weighting factors (w_T) compared to that of the ICRP 60 w_T resulted in a difference in the derived effective dose by up to 0.8 mSv (-20%) in the renal calculus protocol and up to 1.8 mSv (18%) in the pulmonary embolus protocol. This difference is attributed to the reduced radiosensitivity of the gonads and the increased radiosensitivity of breast tissue in the latest ICRP 103 assigned w_T . The results of this study show that the MOSkinTM dosimeter is a useful real-time tool for the direct assessment of organ doses in clinical MSCT examinations.

Keywords

radiation dosimetry, CT, MOSFET, organ dose, tissue weighting factor, ICRP

Organ Point Dose Measurements in Clinical Multi Slice Computed Tomography (MSCT) examinations with the MOSkinTM Radiation Dosimeter

1. Introduction

The MOSkinTM dosimeter, designed at the Centre for Medical Radiation Physics (CMRP), University of Wollongong, Australia, is a radiolucent, easily implementable, real-time radiation dosimetry system built on MOSFET technology (Rozenfeld 2008). It was previously characterised in clinical kilovoltage x-ray photon beams (Lian et al. 2011) and shown to be suitable for the measurement of skin and depth doses in water, with a maximum uncertainty of up to 8% with increasing depth in solid water®.

Conventionally, LiF thermoluminescent (TLD) detectors have been the dosimeter of choice for radiological dosimetry because of their tissue equivalent response (LiF has an atomic number $Z=8.3$ close to that of soft tissue $Z=7.7$). However, the tedious pre-calibration, annealing and post-irradiation readout processes associated with LiF TLD detectors combined with the need for trained dosimetry specialists has been a major hindrance for its adoption in the diagnostic radiology clinic.

Existing quality assurance dose metrics, the Computed Tomography Dose Index (CTDI) and Dose Length Product (DLP), are meaningless for communicating health risk in a typical CT scan. With the increasingly widespread use of CT imaging for medical diagnosis (Brenner and Hall 2007) and to better manage patient perception of high dose CT scans, effective dose is a more patient-centric quantity over CTDI and DLP as it represents a generic estimate of stochastic health risk to a generic model of the human body from a given procedure (McCollough et al. 2010).

The application of MOSFETs for dose measurements in clinical radiology is relatively recent. Peet and Pryor (1999) first used MOSFET technology to measure patient skin entrance doses in diagnostic radiology. Subsequently, Yoshizumi et al. (2007) reported the first successful application of MOSFETs in CT dosimetry. Organ dose assessment with real-time point dosimeters has increasingly become an acceptable method for the derivation of effective dose, as evidenced by previous literature (Hurwitz et al. 2007; Hurwitz et al. 2006; Kawaura et al. 2006; Aoyama et al. 2002).

The main objectives of this study were firstly; to apply the MOSkinTM dosimeter to the measurement of organ point doses in a tissue-equivalent female anthropomorphic phantom for 2 clinical MSCT imaging examinations, namely, the CT renal calculus and the CT pulmonary embolus scans. Secondly, to compare the derived effective doses as a result of the recently introduced ICRP 103 over the ICRP 60 tissue weighting factors (w_T) to our measurements.

2. Materials and Methods

2.1 MSCT Scanner Protocols

A 16-slice General Electric (GE) Discovery 670 NM/CT SPECT/CT scanner was used at 120 kVp tube potential with a measured HVL of 0.8 mm Cu.

Table 1 shows the two clinical imaging protocols which were studied in this work, the CT renal calculus protocol for the detection of renal stones in the pelvic region and the pulmonary embolus protocol for the detection of blood vessel blockage in the chest region.

The scan range for the renal calculus CT examination extended from the upper region of the diaphragm to the pubic symphysis of the anthropomorphic phantom corresponding to a scan length of 250 mm. For the pulmonary embolus CT examination, the scan range extended from the upper end of the lung apex to the lower region of the diaphragm of the anthropomorphic phantom corresponding to a scan length of 300 mm.

Table 1: Imaging parameters for 16-slice MSCT single phasic scan of the abdominal-pelvic region for a renal calculus protocol; and of the chest for a pulmonary embolus (PE) protocol

Imaging Parameters	Protocol name	
	Renal Calculus	PE
Tube potential (kVp)	120	120
Fixed mAs	150	360
Effective mAs ^a	54.5	130.9
Table movement (mm rot ⁻¹)	27.5	27.5
Pitch	1.375	1.375
Detector configuration	16 x 1.25	16 x 1.25
Beam width (mm)	20.0	20.0
Planned scan length (mm)	250	300
Exposed scan length (mm)	278	328
Coverage time (s)	5.05	5.97

^aEffective mAs = $\frac{\text{Average tube current} \times \text{rotation time}}{\text{Pitch factor}}$

2.2 Dosimeter Calibration

The two dosimeters applied in this work were the CMRP MOSkinTM dosimeter and Gafchromic XR-QA2 film (International Specialty Products).

To match as closely as possible the applied CT beam quality and dose levels used in this study, the dosimeters were calibrated in a 150 kVp, HVL=0.63 mm Cu orthovoltage beam on a Gulmay D3300 unit against the Markus parallel plate ionisation chamber (Model N23343, PTW-Frieburg, Germany) with 100 mGy dose delivered to the surface of a solid water® phantom (RMI 457 Gammex, Wisconsin, USA).

2.3 Methodology

The use of a cross-sectional anatomical atlas (Kieffer and Heitzman 1979) enabled us to identify the location of various organs of dosimetric interest throughout the anthropomorphic phantom (The Alderson Radiation Therapy Phantom, Radiology Support Devices, NJ, USA). Within each numbered phantom slab, the detectors were placed within the boundaries of the demarcated organ region to determine average point organ dose as illustrated in Figure 1.

In the scan field-of-view, with the exception of the remainder organs, each recorded organ point dose measurement was the average of 3 individual dosimeter readings. Each point dose measurement was repeated twice to avoid random errors associated with the measurement. For measurement of dose to the remaining organs, each point dose measurement was obtained by a single dosimeter placed in the centroid of the organ.

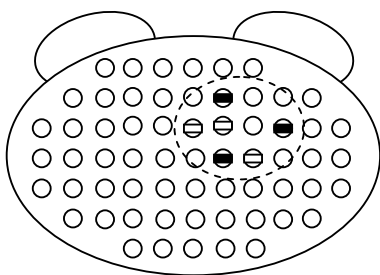


Figure 1: Application of the MOSkinTM (■) and film (□) dosimeters for CT organ point dose measurement in the anthropomorphic phantom. The dotted line demarcates the anatomical position of the heart.

Our preliminary measurements indicated that out-of-field doses, particularly for dose measurements beyond the boundaries of the scan field of view (more than a distance of 5 cm equivalent to 2 slab lengths), lie beyond the low dose detection threshold of both dosimeters

and cannot be reliably measured. As such, the use of the headless phantom in this work was justified as the distances from the primary beam to brain tissue was more than 8 cm.

To overcome the low dose detection threshold of the dosimeters used, we scaled up the technical parameters of the imaging protocols. In the low-dose renal calculus protocol, we doubled the tube current and scanned 3 times before taking a dose measurement. The cumulative dose measured was then scaled down by a factor of 6, to determine organ dose in a single phase MSCT scan. In the case of the pulmonary embolus protocol, we scanned 4 times before taking a dose measurement. The cumulative dose was then scaled down by a factor of 4 to determine organ dose in a single phase MSCT scan.

3. Results

3.1 Depth dose response of dosimeters

The depth dose response of the *MOSkin*TM and film dosimeters were characterized from the surface of the solid water® phantom at an applied surface dose of 100 mGy, to a depth of 100 mm. Figure 2 shows the obtained depth dose characterisation plot. It was found that both the *MOSkin*TM dosimeter and the film dosimeter matched the gold-standard Markus ionisation chamber tissue-equivalent response with a maximum uncertainty of $\pm 10\%$ at 100 mm depth. This uncertainty is acceptable in diagnostic radiology measurements according to the IAEA report (International Atomic Energy Agency 2007) which states that a 20% measurement accuracy is considered acceptable in diagnostic radiology dosimetry where organ doses are low and where the uncertainty for an absolute risk for a stochastic effect is high .

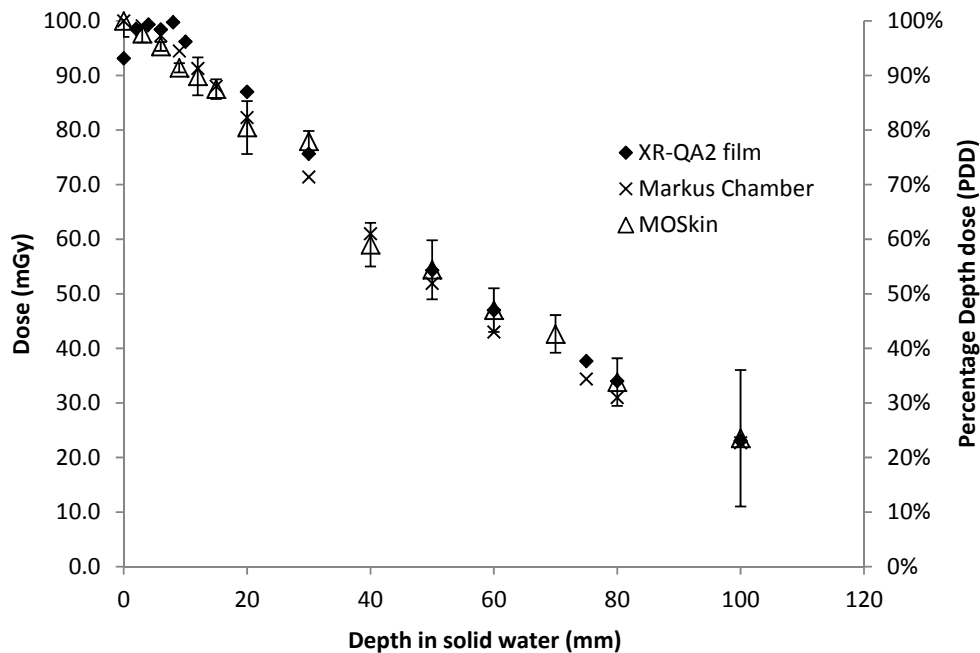


Figure 2: Characterization of the depth dose response of the MOSkinTM dosimeter and film with 100 mGy delivered dose to the surface of the phantom

3.2 Measured Organ doses

Figures 3 and 4 show the results of our organ point dose assessments with the MOSkinTM dosimeter and the Gafchromic XR-QA2 film for the CT renal calculus protocol and the CT pulmonary embolus protocol respectively. Organs in the imaged field of view were found to be in the dose range 4.7 to 9.5 mGy and 16.2 to 27.4 mGy for the renal calculus (RC) and pulmonary embolus (PE) CT scan protocols respectively.

Within the imaged field of view, point doses obtained with the MOSkinTM dosimeter and film compared favourably to within 20% of each other, with the exception of measured average point breast dose (up to 40% difference for the PE protocol) and measured bone surface dose (up to 37% difference for the RC protocol). This difference may be explained by the electronic disequilibrium created by the presence of the air-tissue interface and bone-tissue interface for the assessment of breast dose and bone surface dose respectively.

For doses outside the imaged field of view, particularly at the boundaries of the scan field of view (within 5 mm of the specified scan field), doses recorded by both dosimeters differed by up to 33% for both imaging protocols.

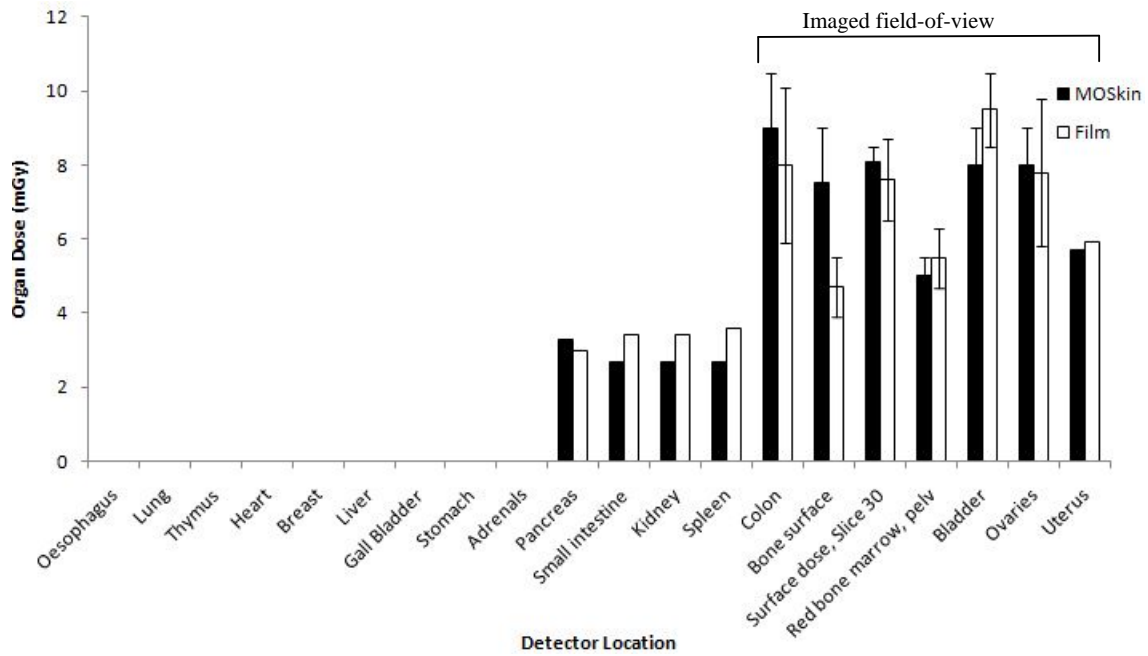
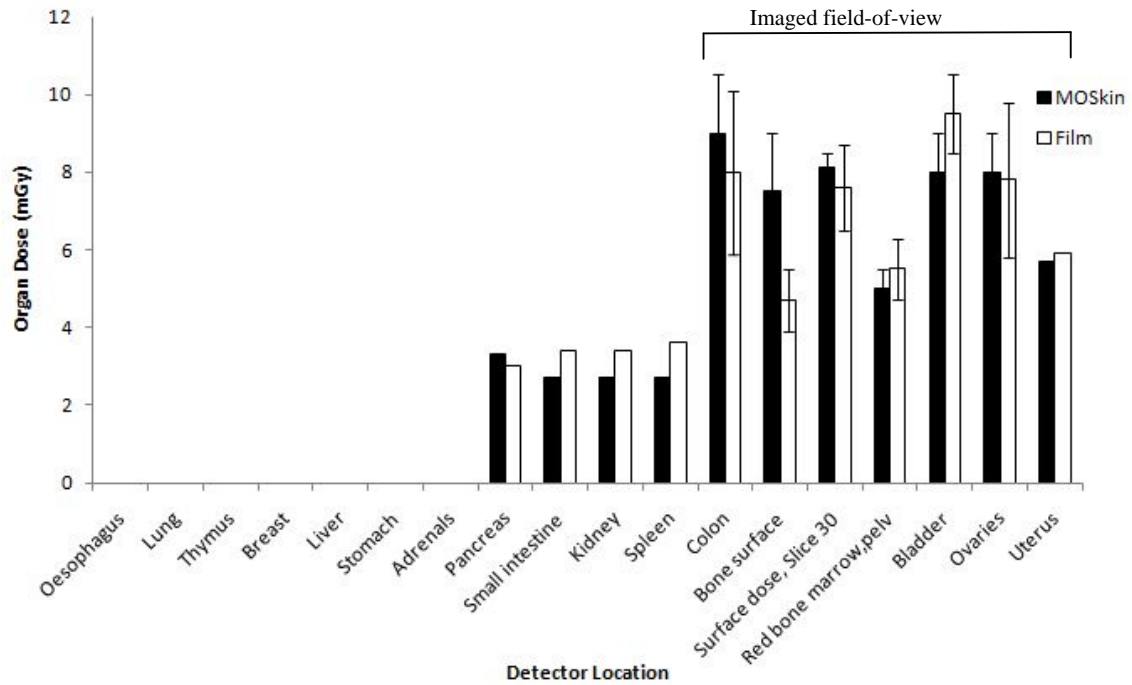


Figure 3: Renal calculus CT imaging scan. Point organ dose measurements obtained with the MOSkinTM dosimeter and Gafchromic XR-QA2 film (a) 18 organ locations of interest as specified in ICRP 60 (b) 20 organ locations of interest as specified in ICRP 103. Error bars refer to the range of dose measurements obtained with 3 individual point dosimeter readouts.

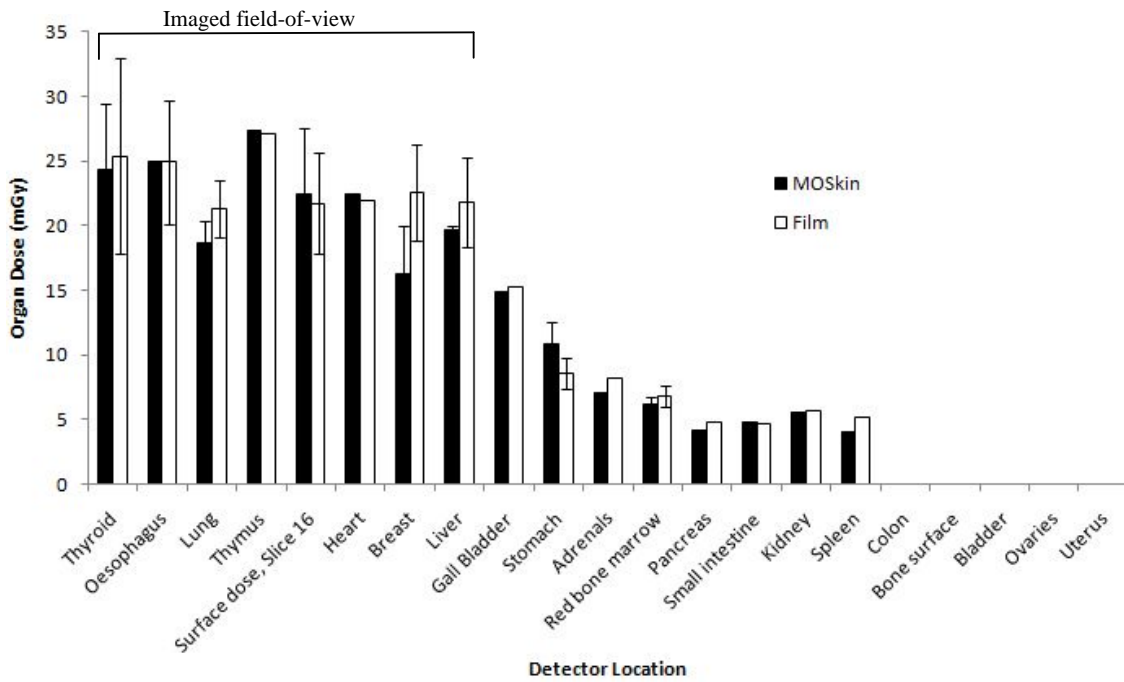
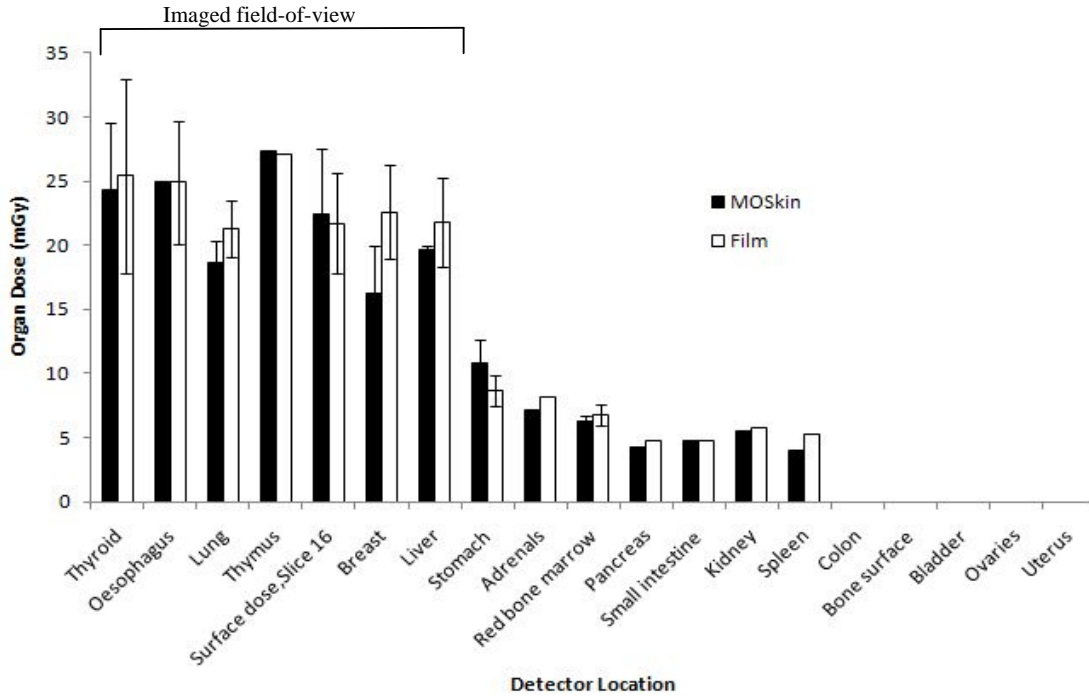


Figure 4: Pulmonary embolus CT imaging scan. Point organ dose measurements obtained with the MOSkin™ dosimeter and Gafchromic XQ-QA2 film (a) 19 organs of interest, ICRP 60 (b) 21 organs of interest, ICRP 103. Error bars refer to the range of dose measurements obtained with 3 individual point dosimeter readouts.

3.3 Evaluation of Effective Dose

Effective dose E is a summation of organ doses multiplied by individual tissue weighting factors. For this study, we used the following equation to derive effective dose E.

$$E = \sum_T w_T \cdot H_T$$

where w_T is the tissue weighting factor and H_T is organ dose measurement in mSv.

For the renal calculus protocol, E was found to be 4.0 mSv and 3.2 mSv when the ICRP 60 and ICRP 103 w_T were respectively applied to measured organ doses. Derived E from film and MOSkinTM point dose measurements were in agreement. The decrease in derived E from 4.0 to 3.2 mSv using E_{103} w_T is primarily due to the recent decrease in the assigned w_T for gonadal tissue (ovaries in the primary scan field of view) from 0.20 in ICRP 60 to 0.08 in ICRP 103.

For the pulmonary embolus protocol, E was found to be 9.2 mSv and 10.6 mSv with the applied ICRP 60 and ICRP 103 w_T respectively. Derived E from film and MOSkinTM point dose measurements agreed to within 10% of each other. The increase in derived E using E_{103} w_T may be explained by the recent increase in the assigned w_T of the radiosensitive breasts in the scan field of view from 0.05 (ICRP 60) to 0.12 (ICRP 103).

4. Discussion and Conclusion

Experimental depth dose characterisation studies done with the MOSkinTM and XR-QA2 film dosimeter showed both dosimeters to be suitable for the assessment of depth doses due to their tissue equivalent response at depth in a clinical kilovoltage beam in the dose range 20 mGy to 100 mGy at a clinical tube potential of 150 kVp (0.63 mm Cu HVL). The MOSkinTM dosimeter has an added advantage over film because of its ability to measure doses in real-time.

Organ doses measured by the MOSkinTM and film dosimeters in this study generally agreed to within 20%. The difference in measured doses is attributed to the changing energy spectrum and dosimeter uncertainties with increasing depth. Larger differences in point dose measurements between the two dosimeters may be attributed to differences in the positioning of the x-ray tube start and end angle due to the CT helical beam not falling on the same organ position on the same point of the arc (Yoshizumi et al. 2007).

We found that the application of ICRP 60 w_T and ICRP 103 w_T to our measured organ doses resulted in a difference in the derived effective dose by up to 0.8 mSv (-20%) in the renal calculus protocol and up to 1.8 mSv (18%) in the pulmonary embolus protocol. This difference is attributed to the reduced radiosensitivity of the gonads and the increased radiosensitivity of breast tissue with the updated ICRP 103 w_T .

Based on the results of this study, we have shown that the MOSkinTM dosimeter is feasible for implementation in the clinical diagnostic x-ray CT setting, with the added advantage of its real-time dose readout capability. Derived effective doses by applying the ICRP w_T to the dosimeter- measured organ doses in an anthropomorphic phantom may lead to improved communication of stochastic health risks to CT patients after taking into account patient specific age-, gender and body habitus.

Acknowledgements

The authors wish to thank Dr Martin Carolan for access to the Gulmay D3300 superficial/ orthovoltage therapy unit for the calibration of dosimeters used in this work.

References

- Aoyama, T., Koyama, S., Kawaura, C., 2002. An in-phantom dosimetry system using pin silicon photodiode radiation sensors for measuring organ doses in x-ray CT and other diagnostic radiology. *Med Phys* 29 (7), 1504-1510.
- Brenner, D., Hall, E., 2007. Computed Tomography — An Increasing Source of Radiation Exposure. *N Engl J Med* 357 (22), 2277-2284.
- Hurwitz, L., Reiman, R., Yoshizumi, T., Goodman, P., Toncheva, G., Nguyen, G., et al., 2007. Radiation dose from contemporary cardiothoracic multidetector CT protocols with an anthropomorphic female phantom: implications for cancer induction. *Radiol* 245 (3), 742-750.
- Hurwitz, L.M., Yoshizumi, T.T., Reiman, R.E., Paulson, E.K., Frush, D.P., Nguyen, G.T., et al., 2006. Radiation Dose to the Female Breast from 16-MDCT Body Protocols. *AJR* 186, 1718-1722.
- International Atomic Energy Agency, 2007. Technical Reports Series no. 457 Dosimetry in Diagnostic Radiology: An International Code of Practice. Vienna.
- International Specialty Products, Product Specification Sheet- Gafchromic XR Series, Wayne, NJ, USA.
- Kawaura, C., Aoyama, T., Koyama, S., Achiwa, M., Mori, M., 2006. Organ and effective dose evaluation in diagnostic radiology based on in-phantom dose measurements with novel photodiode-dosimeters. *Radiat Prot Dosimetry* 118 (4), 421-430.

Kieffer, S.A., Heitzman, E.R., 1979. An Atlas of Cross-Sectional Anatomy: Computed Tomography, Ultrasound, Radiography, Gross Anatomy.

Lian, C.P.L., Othman, M.A.R., Cutajar, D., Butson, M., Guatelli, S., Rosenfeld, A.B., 2011. Monte Carlo study of the energy response and depth dose water equivalence of the MOSkin radiation dosimeter at clinical kilovoltage photon energies. Austral Phys & Eng Sci Med 34 (2), 273-279.

McCollough, C.H., Christner, J.A., Kofler, J.M., 2010. How Effective is Effective Dose as a Predictor of Radiation Risk? AJR 194, 890-896.

Peet, D.J., Pryor, M.D., 1999. Evaluation of a MOSFET radiation sensor for the measurement of entrance surface dose in diagnostic radiology. Br J Radiol 72, 562-568.

Rozenfeld, A.B., 2008. Radiation Sensor and Dosimeter (MOSkin). PCT/AU2008/000788 Australia.

Yoshizumi, T., Goodman, P., Frush, D., Nguyen, G., Toncheva, G., Sarder, M., et al., 2007. Validation of Metal Oxide Semiconductor Field Effect Transistor Technology for Organ Dose Assessment During CT: Comparison with Thermoluminescent Dosimetry. Am J Roentgenol 188 (5), 1332-1336.